

A novel miniaturized loop heat pipe

Yong Tang, Jianhua Xiang, Zhenping Wan^{*}, Wei Zhou, Lei Wu

School of Mechanical and Automotive Engineering, South China University of Technology, Guangzhou 510640, People's Republic of China

article info

Article history:

Received 13 July 2009

Accepted 25 January 2010

Available online 1 February 2010

Keywords:

Miniaturized loop heat pipe

Evaporator

Intensified boiling structure

Condensation structure

Sintered felt wick

abstract

The research on a novel miniaturized loop heat pipe (LHP) consisted of an evaporator, a condenser, vapor and liquid lines is presented in this paper. In the LHP, the evaporator was separated into two parts of boiling and suction chambers by a vapor separator, which drove vapor to one-way flow to vapor line. Moreover, the bottom of evaporator was connected as the cycle channel of refrigerant. Thin copper plates with micro- π s as enhanced structures fabricated by the ploughing–extrusion (P–E) method were embedded in the boiling chamber. Accordingly, the copper fiber sintered felt fabricated by the solid-phase sintering of copper fibers with rough surface, was filled in the suction chamber of evaporator as the wick to provide the capillary force. In addition, the integral rhombic-shaped pillars fabricated by the milling, behaved as intensified condensation structures in the condenser. The startup and operation characteristics of LHP were tested under different heat loads and refrigerants. The experimental results showed that the highest temperature of evaporator reached 93.2 °C under the maximum heat load of 150 W.

© 2010 Published by Elsevier Ltd. All rights reserved.

1. Introduction

Loop heat pipe (LHP), a kind of phase-change heat transfer device, exhibits high heat transfer power, simple structure, light weight, and good adaptability. Comparing with the heat pipe, the LHP can improve more than two orders of magnitude in the ability of heat transfer and solve the problem of θ exible. Therefore, it has been expected as a promising means to solve the heat management problem of the electronics thermal control systems [1,2]. In a LHP, the wicks in the evaporator are usually required to provide the capillary force to drive the cycle of refrigerant and block the vapor to reverse flow into the liquid line at the same time. However, the common wick usually fails to prevent the vapor reverse diffusion into liquid line. In addition, pressure fluctuation happens in the LHP. Thus these features result in a decrease in the performance of LHP.

In recent years, interesting works were focused on developing the thermal control of LHP for high integrated electronics [3–5]. Jie et al. [6] developed a mechanically pumped MLHP with two evaporators about 3 mm in outer diameter. Riehl and Dutra [7] took the acetone as the refrigerant. The experimental results showed that LHP could sustain a temperature of 80 °C when heat load was 70 W. Riehl and Santos [8] put a wick with circumferential grooves into an evaporator, the maximum operational heat load reached 80 W. The evaporator presented heat transfer coef-

icients 60% greater than those verified for the previous capillary evaporator design. Tsai et al. [9] proposed a miniature flat plate LHP with comb grooves evaporator. The test results showed that the flat plate LHP could dissipate heat 50 W and the die temperature was below 90 °C. The glass pipe and stainless steel pipes were used as evaporator section in the LHP [10]. The experimental results showed that the heat transfer was enhanced greatly due to the combined effect of the evaporation. Singh et al. [11] designed a LHP with the flat disk shape evaporator with 10 mm in thickness and 30 mm in diameter, which was made of copper plate, and nickel was used as wick. The device was able to transfer the maximum heat load of 70 W with evaporator temperature below 100 ± 5 °C. The thermal resistance of LHP was between 0.17 and 5.66 °C/W. Joung et al. [12] designed and adopted a planar bifacial wick structure for the LHP with flat bifacial thermo-contact surfaces with active area of 25 cm². The LHP showed a minimum thermal resistance of 1.27 °C/W at the maximum heat load of 78 W, while the temperature of the evaporator reached 124.1 °C.

In this study, we developed a novel LHP with an evaporator, a condenser, vapor and liquid lines. In the evaporator, a vapor separator was designed to separate the evaporator into two parts of boiling and suction chambers. The vapor separator could drive vapor to one-way flow to vapor line. The copper fiber sintered felt was used as wick. Accordingly, the thin copper plates with orthogonal micro- π s as the enhanced boil structure and integral rhombic pillars as condensation structures were embedded into the evaporator and the condenser. In addition, the effect of power inputs and refrigerants on the dynamic performances of LHP was investigated in detail.

^{*} Corresponding author. Tel./fax: +86 20 87114634.

E-mail address: zhpwan@scut.edu.cn (Z. Wan).

2. Fabrication of miniature LHP

The miniature LHP was constructed with four parts: an evaporator, a condenser, vapor line and liquid line. Fig. 1 shows the structure diagram of LHP system. When the evaporator was heated, the refrigerant began to vaporize and flow toward the condenser along the vapor line. Later, the refrigerant would experience a phase change to liquid. Finally, the condensed liquid returned to evaporator through the liquid line. The evaporator was designed into the rectangular shape ($L \times W \times H = 55 \text{ mm} \times 50 \text{ mm} \times 18 \text{ mm}$). The dimension of condenser was 76 mm in length, 80 mm in width, and 95 mm in height. The material of the evaporator and the condenser was red copper and aluminum, respectively. Two PU tubes ($\varnothing 10 \text{ mm} \times 8 \text{ mm}$, $\varnothing 8 \text{ mm} \times 6 \text{ mm}$) about 350 mm in length were served as vapor and liquid lines, respectively.

2.1. Fabrication of evaporator and its components

The miniaturized LHP performed insufficient power dissipation capacity as a result of the reduction size. Accordingly, the phase

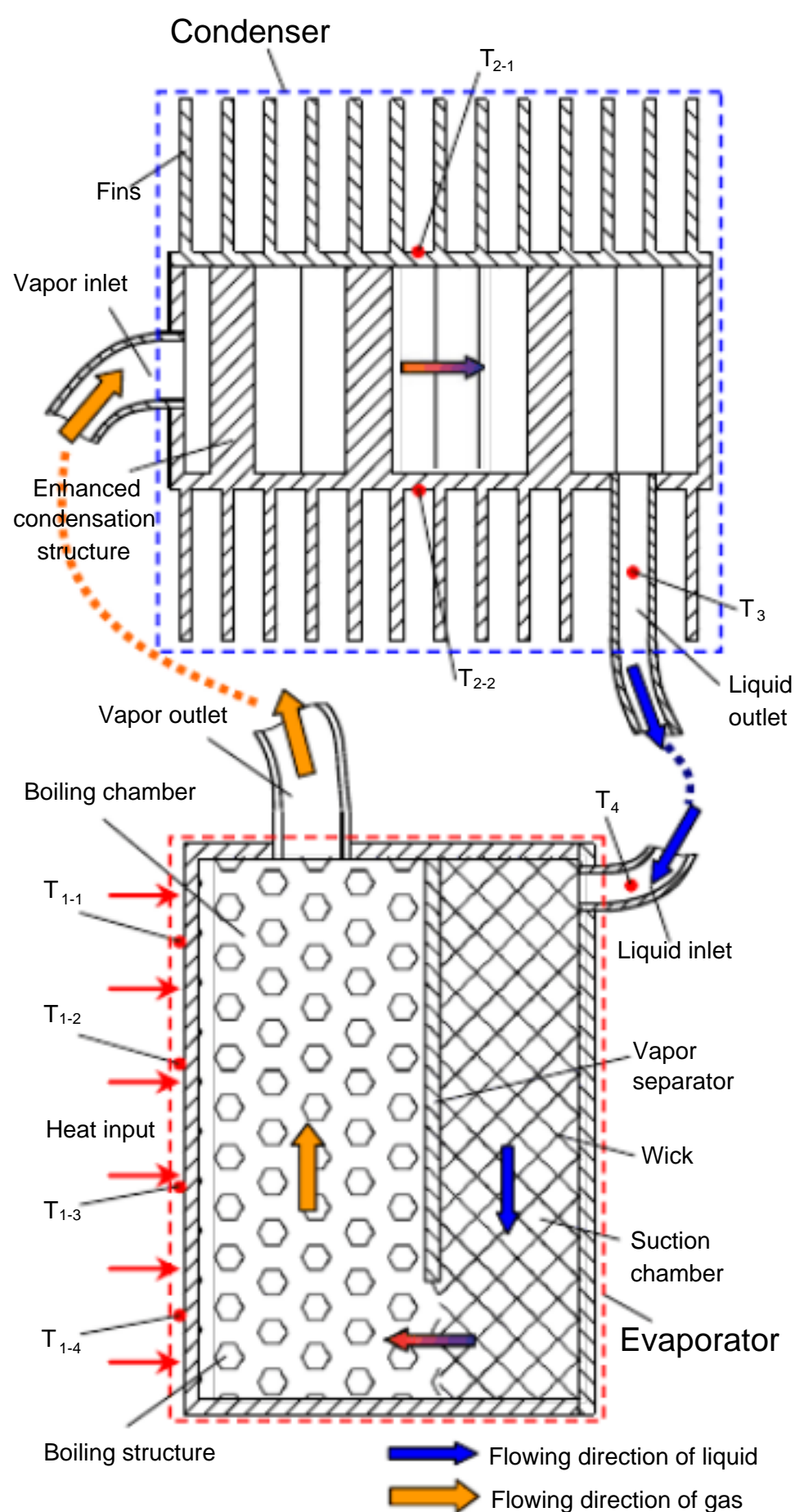


Fig. 1. Schematic diagram of LHP system.

change became difficult to keep boiling for the thin wick of the miniaturized LHP in the evaporation process [13]. In this study, the evaporator was separated into two parts of boiling and suction chambers by a vapor separator (shown in Fig. 2). The bottom of evaporator was connected to ensure the cycle of refrigerant, and meanwhile, the one-way flow of vapor was achieved due to the barrier function of the vapor separator. These structures were different from the traditional LHP which usually used the wick to obstruct the backflow of the refrigerant [14,15].

2.1.1. Forming process of micro- \varnothing n on thin copper plate

Nimkar et al. [16] validated that micro-grooves, cracks, and \varnothing ns can speed up the vaporization of refrigerant, resulting in the significant improvement in the boiling performance. To improve the heat transfer performance, Tang et al. [17,18] studied on the processing methods of micro-grooves, cracks, and \varnothing ns. In this study, the orthogonal ploughing–extrusion (P–E) method was used to fabricate the thin copper plate with micro- \varnothing ns. The material of P–E tool was W18Cr4V. The P–E tool included a ploughing edge, a primary extrusion face A_r , a minor extrusion face A_r^0 , a primary forming face A_b and a minor forming face A_b^0 (shown in Fig. 3 a). The $P_0 - R_0$ cross-section of the tool was a wedge structure (α_0 – tool clearance of P–E tool, K_r – edge inclination angle, b – major forming angle, b^0 – minor forming angle, r_0 – major extrusion angle, r_0^0 – minor extrusion angle). The blade in the front end of wedge structure can plough the metal and drive the metal flow along the major extrusion face and the minor one. The micro- \varnothing n was formed by the main extrusion face, and then was trimmed by the minor face to higher.

The experiment was carried out on the planer (No. B6050B). The parameters of P–E tool was $K_r = 80^\circ$; $\alpha_0 = 10^\circ$; $r_0 = 30^\circ$; $r_0^0 = 10^\circ$; $b = 15^\circ$; $b^0 = 5^\circ$. The process procedure was described as follow: firstly, parallel micro-grooves was obtained on the surface of copper plate by the longitudinal P–E, then the micro-cracks and micro-hole were achieved by extruding the grooves formed in the first step by the second P–E in the vertical direction, as shown in Fig. 3b.

Thin copper plate of 0.4 mm in thickness with micro- \varnothing ns and cracks is shown in Fig. 3c. The depth and width of micro-groove was 0.25 mm and 0.40 mm, respectively. The height of micro- \varnothing n was 0.10 mm. The surface with micro-grooves and micro-cracks played an important role on improving the performance of evaporator. Thin copper plates were parallel-embedded in the boiling chamber to increase the evaporation area greatly.

2.1.2. Fabrication of copper fiber sintered felt

Metal fibers sintered felt is a new type kind of porous metal materials, which is fabricated by the sintering of metal fiber instead of metal powder. The metal fiber sintered felt have the

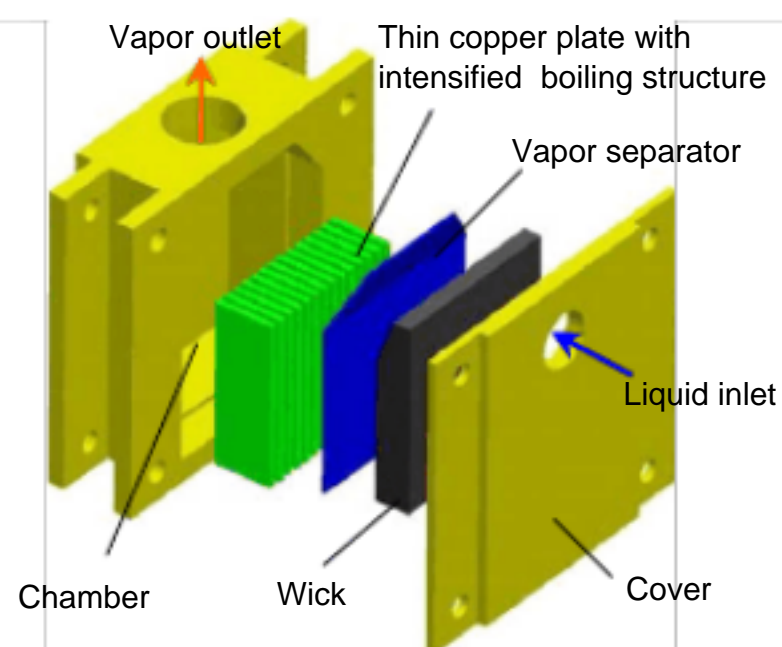


Fig. 2. Schematic diagram of evaporator.

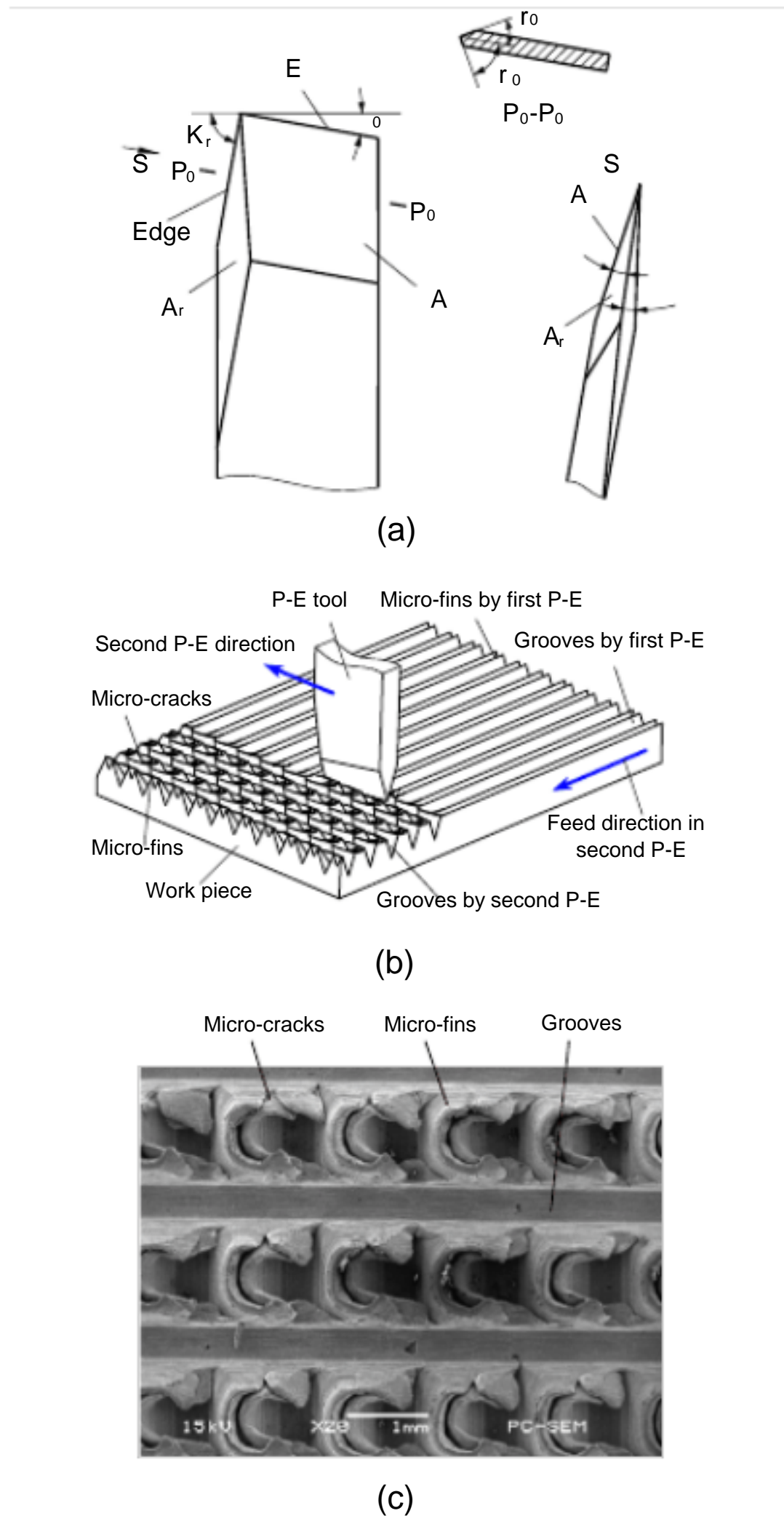


Fig. 3. (a) P-E tool, (b) manufacturing process and (c) SEM image of micro-fins on thin copper plate (a_0 – tool clearance of P-E tool, K_r – edge inclination angle, b – major forming angle, b^0 – minor forming angle, r_0 – major extrusion angle, r_0^0 – minor extrusion angle).

porous structure of three-dimensional network, high-precision and full-connectivity pore size, high porosity and large specific surface area [19 – 21]. So, these features of metal fiber sintered felt provide a promising application as the wick.

In this study, the copper fiber was fabricated by the cutting method using the multi-tooth tool on a horizontal lathe (No. C6132A). The parameters and shape of tool are shown in Fig. 4a. The main cutting blade was composed of many tiny teeth. The distance and height of tiny teeth were 0.3 mm and 0.2 mm, respectively. C_1 was nominal rake angle, a_1 was nominal clearance angle, in this study, $C_1 = 30^\circ$, $a_1 = 8^\circ$.

Fig. 4b shows the SEM image of copper fiber fabricated by the cutting method. It is noted that the copper fiber has a rough

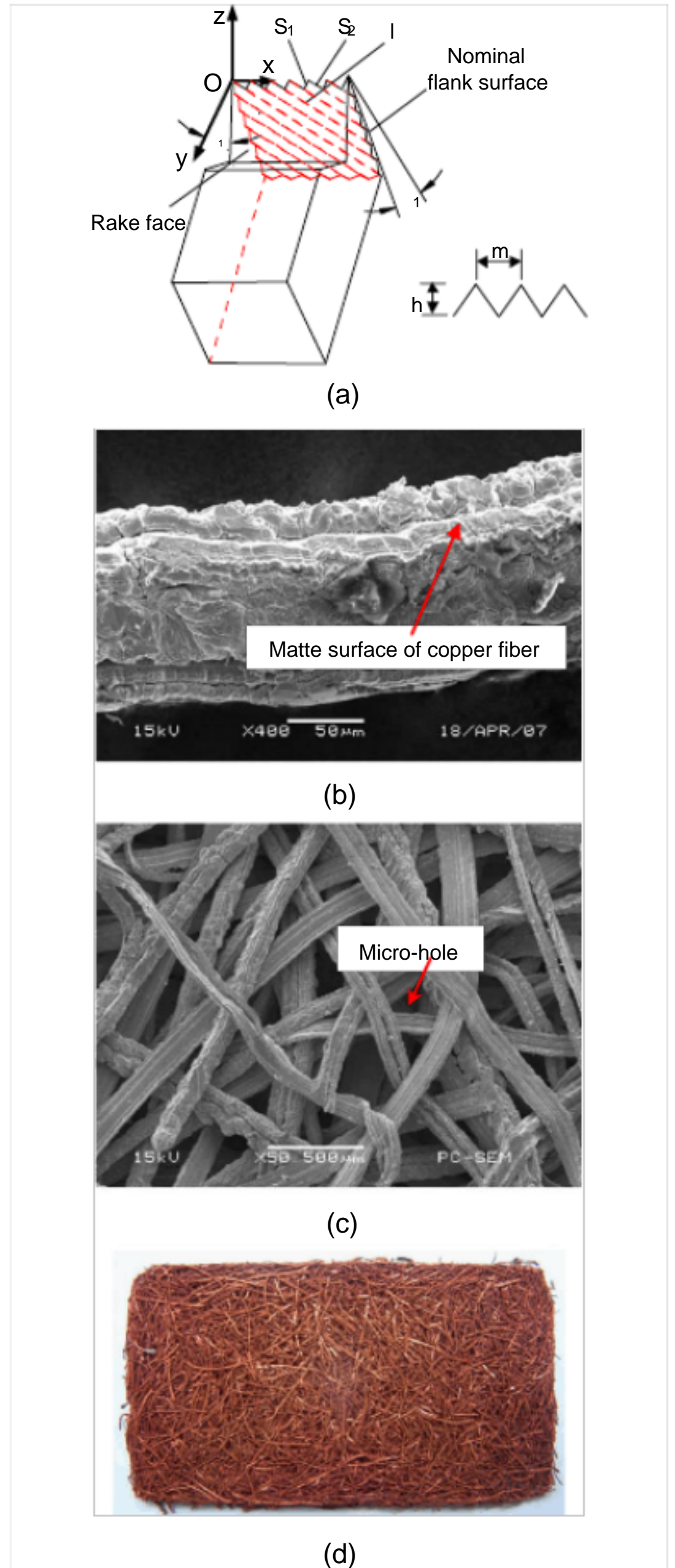


Fig. 4. (a) Multi-tooth tool, (b) SEM image of copper fibers, (c) and (d) SEM image and shape of sintered felt (C_1 – nominal tool side rake, a_1 – nominal tool clearance, S_1 , S_2 , I – tool edge, m – tooth pitch, h – tooth depth).

surface, so the specific surface area was increased. This feature creates the advantages for sintering copper fiber. The copper fiber sintered felt was obtained by the solid-phase sintering of copper fibers. The SEM and optical images of copper fiber sintered felt is

shown in Fig. 4c and d, respectively. The copper fiber sintered felt with 70% porosity was used as wick in the suction chamber. The porosity of metal fiber sintered felt was calculated by the following equation:

$$\epsilon = 1 - \frac{M}{\rho V} \times 100\% \quad (1)$$

M – the mass of the copper fiber sintered felt (g), V – the volume of the copper fiber sintered felt (cm^3), ρ – the density of red copper (g/cm^3).

2.2. Fabrication process of condenser

High condensation efficiency is crucial to the power dissipation capacity for the miniaturized LHP. In this study, the integral condensation structure of staggered pillar with rhombic-shaped section was fabricated by the milling method on a milling machine (No. X5032). The forming process of integral condensation structure is shown in Fig. 5a. The staggered integral pillar structure located in the bottom of condenser and outside integral fins was used as intensified condensation structure. These structures are conducive to increase the condensation area and decreased the thermal resistance, so the heat transfer coefficient can be increased. The inside integral pillar structure and appearance of condenser is shown in Fig. 5b and c, respectively.

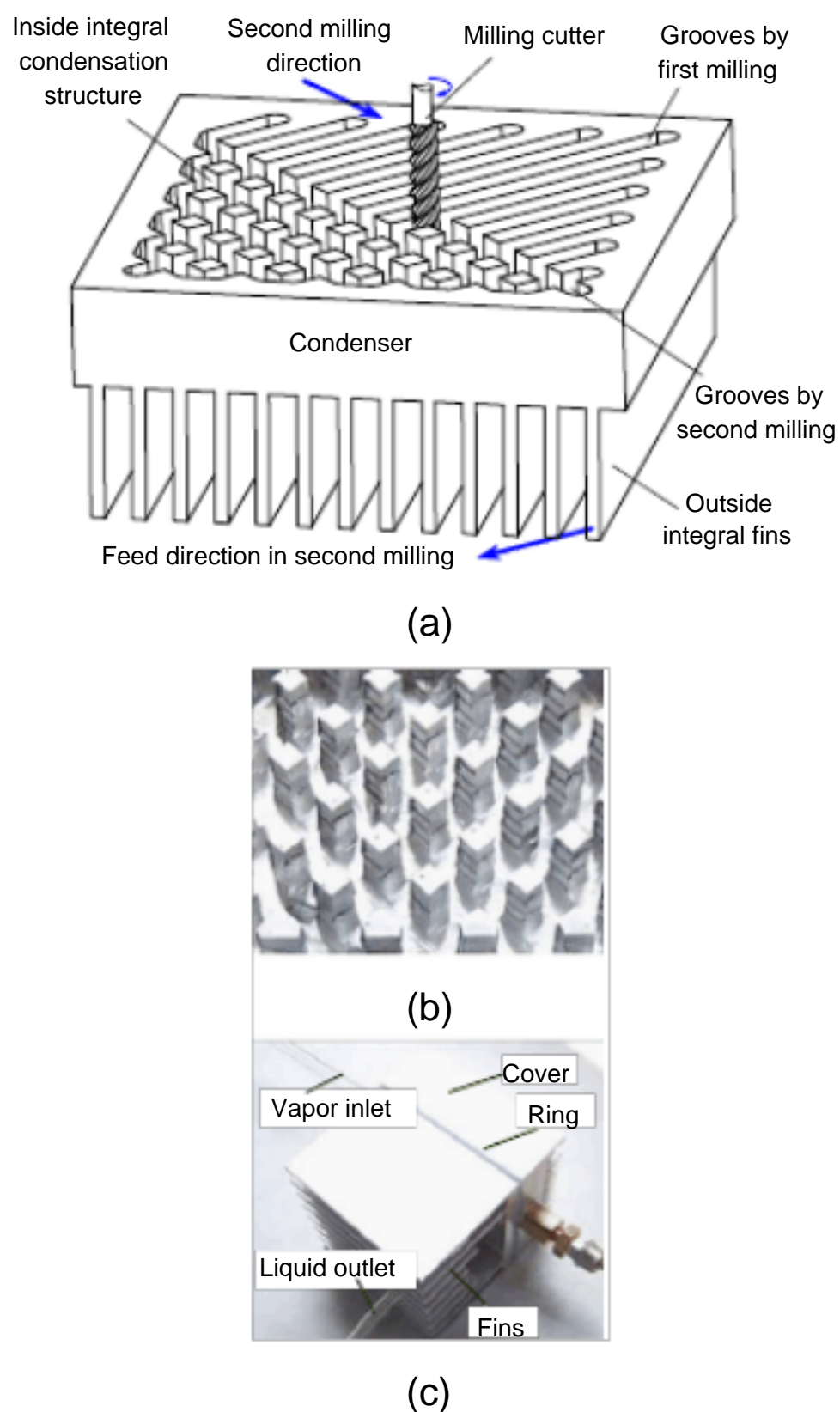


Fig. 5. (a) Scheme diagram of integral condensation structure process, (b) integral pillar structure and (c) shape of condenser.

3. Testing system of LHP

The testing system was built to evaluate the performance of LHP, including three parts: heater, cooler and temperature data collection (shown in Fig. 6). The heater part consisted of a heater and a voltage regulator. To prevent the heat loss, firstly, the solid copper plate with 50 mm × 50 mm × 15 mm in dimension embedded with four resistors of 400 Ω used as heat source was fastened on the evaporator by mechanically, then the solid copper plate was wrapped with asbestos tightly, later was placed into a wooden box. The heat loss was produced from vapor line and liquid line mainly (Line material: PU) can be ignored, because the amount of heat loss was very small. The heat generated from resistors could be controlled by a voltage regulator. So the heat source was calculated by the following equation:

$$Q = \frac{U^2}{R_t} \quad (2)$$

where Q was input power (W), U was voltage (V), R_t was total resistance (Ω).

Four resistors of 400 Ω was parallel connection, so R_t was calculated:

$$R_t = \frac{1}{\frac{1}{R_1} + \frac{1}{R_2} + \frac{1}{R_3} + \frac{1}{R_4}} \quad (3)$$

So, when $U = 70.7$ V, input power was 50 W. The relationship of voltage and power was shown in Table 1.

A fan as cooler part located in the outside of condenser to force air convection. The rotating speed of fan was 2200 r/min. The temperature data collection part were made up of temperature measuring module ADAM-4018, analog/digital (A/D) convertor ADAM-4502, eight K type thermocouples, and a computer. Temperature signal was transmitted to A/D convertor from temperature measuring module which was connected with the thermocouples, and then to computer whose signal sampling frequency was 1 datum s^{-1} . The eight thermocouples were distributed on the evaporator ($T_{1-1}, T_{1-2}, T_{1-3}, T_{1-4}, T_1 = (T_{1-1} + T_{1-2} + T_{1-3} + T_{1-4})/4$) the condenser ($T_{2-1}, T_{2-2}, T_2 = (T_{2-1} + T_{2-2})/2$), liquid outlet (T_3), and liquid inlet (T_4) (shown in Fig. 1).

4. Results and discussion

The temperature and thermal resistance of LHP were tested under the different heat loads and refrigerants. The refrigerants had a

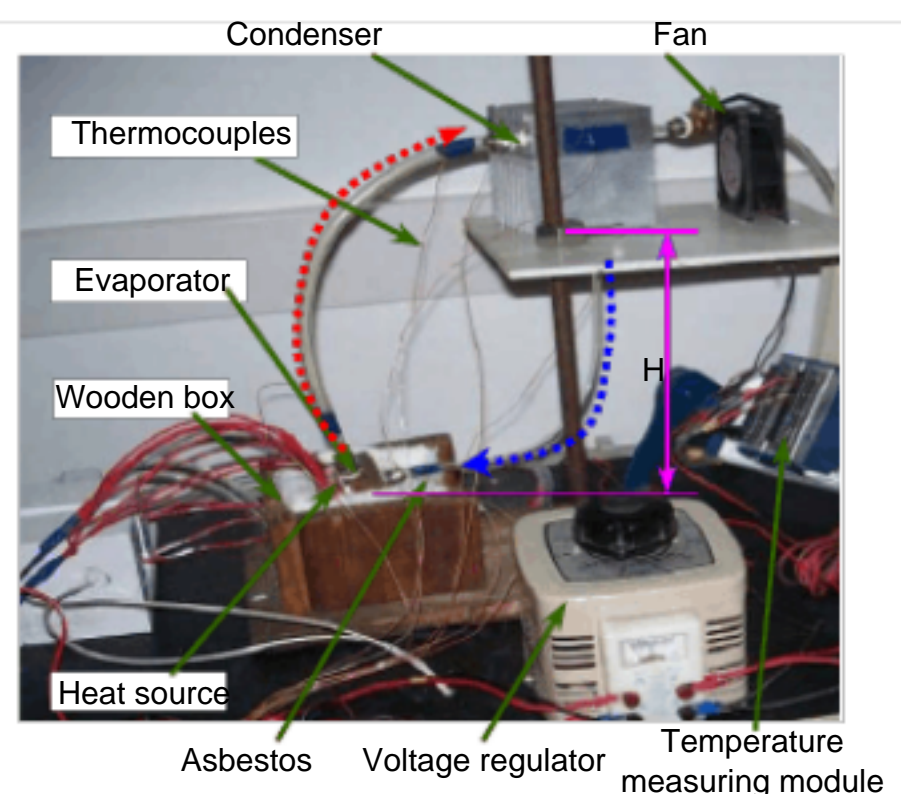


Fig. 6. Performance test system of LHP.

Table 1
Relationship of voltage and input power.

Voltage (V)	Input power (W)
70.7	50
86.6	75
100	100
122.5	150

significant influence on the performance of LHP. Excessive of refrigerant can cause the increase in the temperature of evaporator or even the disability of LHP, and vice versa. Generally, the optimal inventory of the refrigerant was at 40–50% of inner volume of LHP [22]. Therefore, the amount of refrigerant was determined as 20 ml according to the inner volume of LHP. In order to decrease the starting temperature, the pressure of LHP system was decreased to 200 Pa by a vacuum pump.

4.1. The effect of power input on the dynamic characteristics

Ethanol with 99.5% in concentration was used as refrigerant. The copper fiber sintered felt with 70% porosity was used as wick in the suction chamber. Fig. 7a–d shows the startup and running characteristics of LHP under the power input of 50 W, 75 W, 100 W and 150 W, respectively.

The startup and running characteristics of LHP were divided into four stages according to Fig. 7. The first stage was named the rising temperature stage of evaporator. In this stage, majority heat was absorbed by the shell of evaporator, no enough heat made the refrigerant boil. In the second stage, a small portion of refrigerant started to vaporize, and then condensed quickly by the vapor tube. The first and second stages experienced a short time. The

third stage was named the stage of intense boiling. A large number of vapor entered into the condenser through the vapor line, while the temperature of system was rising. It was a long time duration in this stage. Moreover, the experimental result showed that the LHP could not work without a vapor separator in the evaporator, because the liquid could not reach the thin copper plate to vaporize under the pressure of the vapor to wick. The last stage, the temperature of LHP system kept stable situation. In the LHP system, the temperature was gradually reduced from the evaporator to condenser along the vapor line. Because the temperature of liquid inlet (T_4) was affected by heat conduct from capillary and evaporator wall, T_4 and T_3 were approximately equal. So $T_1 - T_4$ meets the following relationship:

$$T_1 > T_2 > T_3 \quad \text{and} \quad T_1 > T_2 > T_4 \quad \text{e4T}$$

Fig. 7a shows that the temperature of the evaporator is increased quickly and the temperature of the condenser is kept at 25 °C. When the temperature of evaporator approached 29.9 °C, the LHP started to startup. The temperature of evaporator raised up slowly and then kept at 47.1 °C at last. The temperature of the condenser raised up at initial startup, then slightly increased and was constant 42 °C finally. When the LHP began to work, boiling and bubbles happened in the evaporator because vapor flowed from the evaporator to vapor line. When the heat load was increased to 75 W or 100 W, the boiling time was shortened (as shown in Fig. 7b and c). When the heat load was 150 W, the startup and operating characteristics of LHP were showed in Fig. 7d. The evaporator temperature was increased continuously and later was kept at 93.7 °C, which was the highest temperature approached allowable operation temperature for electronic components. These results indicate that LHP is capable of dissipating 150 W of thermal energy and keeping the evaporator temperature under 100 °C.

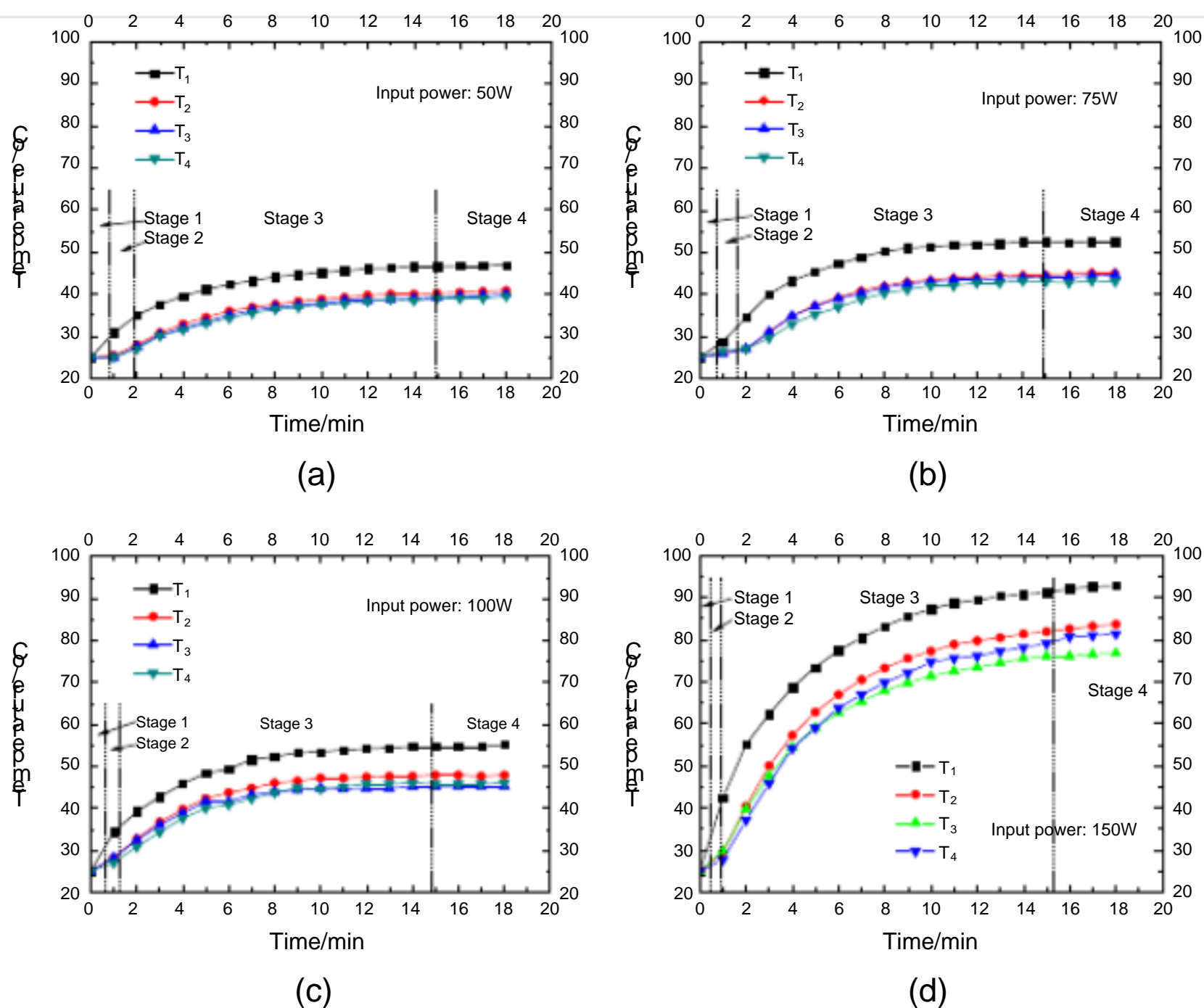


Fig. 7. Transient state response of LHP under different heat loads with alcohol as refrigerant.

4.2. The effect of refrigerant on the dynamic characteristics

Fig. 8a–d shows the startup and run characteristics of LHP with pure water as refrigerant at the power input of 50 W, 75 W, 100 W and 150 W, respectively. Since the specific heat capacity and boiling point of water in vacuum are higher than that of alcohol, more amount of heat is required to be absorbed by water to boiling under the same condition. The same phenomenon that LHP could not work without a vapor separator in the evaporator appeared when alcohol was used as refrigerant, because there is not the cycle of refrigerant. Comparing Fig. 7 to Fig. 8, it is found that the startup time of water as refrigerant is three times longer than alcohol. However, it takes the same time length for the system to reach the steady state.

The rising temperature of the evaporator and condenser with water as refrigerant was higher than that with alcohol in low heat load situation (0–75 W), but the reverse result was obtained in the case of high heat load situation (75–150 W). Interestingly, the total time of three stages was equal with alcohol or water as refrigerant for the LHP.

4.3. Thermal resistance of LHP

The highest temperature of evaporator with water as refrigerant was higher than that of alcohol in the low heat load condition, because the specific heat capacity of water is higher than alcohol. However, the reverse was the case when the input power increased to 150 W. Thermal resistance is calculated as following equation:

$$R = \frac{T_{\text{evp}} - T_{\text{con}}}{Q_{\text{in}}} \quad (5)$$

T_{evp} – temperature of evaporator (°C), T_{con} – temperature of condenser (°C), Q_{in} – heat load (W).

When water and alcohol were used as refrigerants respectively, the thermal resistance of LHP system was decreased with increasing heat load (shown in Table 2). Furthermore, the thermal resistance of system varied under different refrigerants and heat loads. When the heat load was increased to 73 W, thermal resistance was equal under the different refrigerants. The low thermal resistance could be achieved in case of alcohol as refrigerant under the low input power. Also, the water as refrigerant behave better for the heat transfer of large heat density.

5. Conclusions

- (1) A novel LHP with a vapor separator in the evaporator was designed and fabricated in this study. The vapor separator insured the one-way flow of refrigerant in order to achieve a stable heat transfer performance of LHP. It gives a new way to resolve the contradiction between power dissipation capacity and miniaturization for the LHP.
- (2) The thin copper plate with micro-grooves, cracks, and fins on the surface, which was used as the strengthened boiling structure, was fabricated by the P–E method. The copper fiber sintered felt as wick, fabricated by the solid-phase sintering of copper fibers with rough surface, provided the capillary force for the LHP. The staggered integral pillar with rhombic-shaped section processed by the milling method was used as the intensified condensation structure.
- (3) The LHP exhibited a good startup performance and adaptive capacity of extended input power under the different working conditions. When the alcohol was used as refrigerant, the LHP demonstrated better heat transfer performance under the low input power. However, the water was optimal

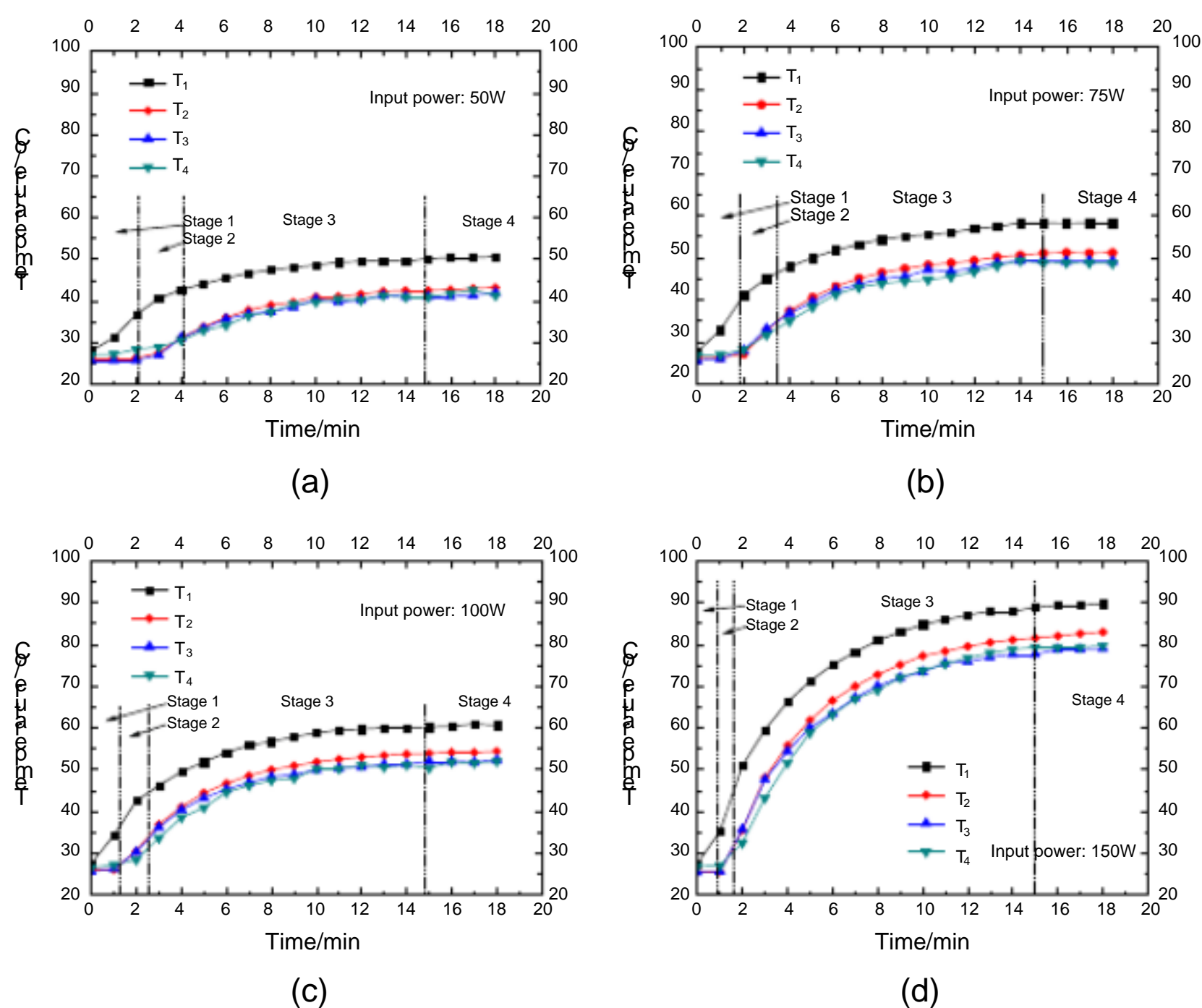


Fig. 8. Transient state response of LHP under different heat loads with water as refrigerant.

Table 2
Thermal resistance of LHP system.

Heat load (W)	Thermal resistance	
	Alcohol as refrigerant (°C/W)	Water as refrigerant (°C/W)
50	0.1200	0.1480
75	0.0990	0.0960
100	0.0700	0.0680
150	0.0455	0.0315

refrigerant for the LHP under the high power input condition. A minimum thermal resistance was 0.0315 K/W under the maximum heat load of 150 W with water as refrigerant in the LHP. In addition, the temperature of evaporator reached 93.7 °C when alcohol was used as refrigerant under the maximum heat load.

Acknowledgements

This research were supported by the National Nature Science Foundation of China (Nos. 50436010, 50605023, 50675070 and U0834002), and the Natural Science Foundation of Guangdong Province (No. 07118064).

References

- [1] Yury F. Maydanik, Loop heat pipes, *Applied Thermal Engineering* 25 (5 – 6) (2005) 635 – 657.
- [2] Yury F. Maydanik, Sergey V. Vershinin, Mikhail A. Korukov, Jay M. Ochterbeck, Miniature loop heat pipes – a promising means for cooling electronics, *IEEE Transactions on Components and Packaging Technologies* 28 (2) (2005) 290 – 295.
- [3] Yuming Chen, Manfred Groll, Rainer Mertz, Yu F. Maydanik, S.V. Vershinin, Steady-state and transient performance of a miniature loop heat pipe, *International Journal of Thermal Sciences* 45 (11) (2006) 1084 – 1090.
- [4] Vladimir G. Pastukhov, Yury F. Maydanik, Low-noise cooling system for PC on the base of loop heat pipes, *Applied Thermal Engineering* 27 (5 – 6) (2007) 894 – 901.
- [5] V.G. Pastukhov, Yu F. Maydanik, C.V. Vershinin, M.A. Korukov, Miniature loop heat pipes for electronics cooling, *Applied Thermal Engineering* 23 (9) (2003) 1125 – 1135.
- [6] Liu Jie, Pei Nian-Qiang, Guo Kai-Hua, He Zhen-Hui, Li Ting-Xuen, Experimental investigation on a mechanically pumped two-phase cooling loop with dual-evaporator, *International Journal of Refrigeration* 31 (7) (2008) 1176 – 1182.
- [7] Roger R. Riehl, Thiago Dutra, Development of an experimental loop heat pipe for application in future space missions, *Applied Thermal Engineering* 25 (1) (2005) 101 – 112.
- [8] Roger R. Riehl, Nadjara dos Santos, Loop heat pipe performance enhancement using primary wick with circumferential grooves, *Applied Thermal Engineering* 28 (14 – 15) (2008) 1745 – 1755.
- [9] Meng-Chang Tsai, Chun-Sheng Yu, Shung-Wen Kang, Flat plate loop heat pipe with a novel evaporator structure, in: *Proceedings of 21st Annual IEEE Semiconductor Thermal Measurement and Management Symposium*, San Jose, CA, USA, 15 – 17 March, 2005, pp. 187 – 190.
- [10] Jie Yi, Zhen-Hua Liu, Jing Wang, Heat transfer characteristics of the evaporator section using small helical coiled pipes in a looped heat pipe, *Applied Thermal Engineering* 23 (1) (2003) 89 – 99.
- [11] Randeep Singh, Aliakbar Akbarzadeh, Masataka Mochizuki, Operational characteristics of a miniature loop heat pipe with flat evaporator, *International Journal of Thermal Sciences* 47 (11) (2008) 1504 – 1515.
- [12] Wukchul Joung, Taeu Yu, Jinho Lee, Experimental study on the loop heat pipe with a planar bifacial wick structure, *International Journal of Heat and Mass Transfer* 51 (7 – 8) (2008) 1573 – 1581.
- [13] Hung-Yi Li, Kuan-Ying Chen, Thermal performance of plate-fin heat sinks under confined impinging jet conditions, *International Journal of Heat and Mass Transfer* 50 (9 – 10) (2007) 1963 – 1970.
- [14] E. Bazzo, R.R. Riehl, Operation characteristics of a small-scale capillary pumped loop, *Applied Thermal Engineering* 23 (6) (2003) 687 – 705.
- [15] Jianlin Yu, Hua Chen, Hua Zhao, Yanzhong Li, An experimental investigation on capillary pumped loop with the meshes wick, *International Journal of Heat and Mass Transfer* 50 (21 – 22) (2007) 4503 – 4507.
- [16] Nitesh D. Nimkar, Sushil H. Bhavnani, Richard C. Jaeger, Effect of nucleation site spacing on the pool boiling characteristics of a structured surface, *International Journal of Heat and Mass Transfer* 49 (17 – 18) (2006) 2829 – 2839.
- [17] Y. Tang, Y. Chi, Z.-P. Wan, X.-K. Liu, J.-Ch. Chen, X.-X. Deng, L. Liu, A novel micro-groove array structure and forming process, *Journal of Materials Processing Technology* 203 (1 – 3) (2008) 548 – 553.
- [18] Jian-hua Xiang, Yong Tang, Bang-yan Ye, Wei Zhou, Hui Yan, H.U. Zhi-hua, Compound forming technology of outside 3D integral fin of copper tubes, *Transactions of Nonferrous Metals Society of China* 19 (2) (2009) 335 – 340.
- [19] Richard R. Williams, Daniel K. Harris, The heat transfer limit of step-graded metal felt heat pipe wicks, *International Journal of Heat and Mass Transfer* 48 (2) (2005) 293 – 305.
- [20] Yong Tang, Wei Zhou, Mingqiang Pan, Hongqing Chen, Wangyu Liu, Hao Yu, Porous copper fiber sintered felts: an innovative catalyst support of methanol steam reformer for hydrogen production, *International Journal of Hydrogen Energy* 33 (12) (2008) 2950 – 2956.
- [21] Z.P. Wan, Y. Tang, Y.J. Liu, W.Y. Liu, High efficient production of slim long metal fibers using bifurcating chip cutting, *Journal of Materials Processing Technology* 189 (1 – 3) (2007) 273 – 278.
- [22] Pin-Chih Chen, Wei-Keng Lin, The application of capillary pumped loop for cooling of electronic components, *Applied Thermal Engineering* 21 (17) (2001) 1739 – 1754.